A Frequency Dividing Control Method Using Wavelet for Active Magnetic Bearing System

Xuan Yao [a], Zhaobo Chen [b], Xiaoxiang Liu [c]

[a] School of Mechatronics Engineering, Harbin Institute of Technology, No.92 West Dazhi Street, Harbin, China
[b] School of Mechatronics Engineering, Harbin Institute of Technology, No.92 West Dazhi Street, Harbin, China, chenzb@hit.edu.cn
[c] Beijing Institute of Control Engineering, South Beijing Haidian area three streets 16, Beijing, China, monkeyfiona@163.com

***Abstract*—Benefiting from the features such as zero-friction and active control, Active magnetic bearings (AMBs) have several advantages over conventional mechanical bearings and are getting more applications. Various control strategies and algorithms have been applied and designed to deal with the nonlinear characteristic as well as the complex rotor dynamics. However, most control schemes are in time domain, while the control in frequency domain, which is also essential for stability of rotor system, is rarely considered. In this paper, a frequency dividing control method is proposed for AMB-rotor system. Wavelet theory is applied for frequency dividing control. The control scheme is implemented by filter banks for Wavelet Transform (WT) and a group of PID controllers for multi-frequency control. Simulation on a 4-DOF AMB-rotor system in different cases is run and vibration of the system is analyzed. Simulation results demonstrate that the proposed approach has an obvious control effect with better precision and quicker response than conventional PID control. This research provides a time-frequency control approach for AMBs, and this low-hardware-cost approach can also be adopted in other vibration control, especially in multi-frequency applications.**

I. INTRODUCTION

Active magnetic bearings (AMBs), which are high-tech support means, are used in more applications for rotating machinery. AMBs have several advantages over conventional mechanical bearings because of their unique features such as zero-friction and active control [1]. However, due to the nonlinear characteristics of electromagnetic principle and complex rotor dynamics, it is not easy to provide suitable control. Various control strategies and algorithms have been applied and designed [2,3]. Most control schemes are in time domain, while the control in frequency domain, which is also essential for stability, is rarely considered. Since the frequency components of rotor system are usually complicated, the control schemes which take frequency-domain control into account, should be brought to the forefront.

LMS (Least mean square) algorithm based adaptive feedforward control is an effective approach in vibration control. Since the input of this algorithm is a time series of signals, control in frequency domain is also involved. Wei et. al. designed a control law based on block normalized least mean square algorithm for an electromagnetic suspension vibration isolator [4]. Plaza and Pawelczyk proposed a LMS-IMC (Internal Model Control) algorithm for weighted minimum variance control of AMB system [5]. Kang and Yoon used a feedforward compensator by means of filtered-x LMS algorithm to attenuate disturbance responses subjected to base motion in AMB system [6].

Frequency dividing control is an attractive approach for frequency-domain control. This method can divide the feedback signals of the system in frequency domain and provides different control strategy or different controller parameters for the divided frequency. Tzes and Kyriakides proposed a hybrid frequency-time domain control scheme for flexible link manipulators. Their controller is an adaptive fuzzy controller based on a frequency domain identification algorithm [7]. Luo et. al. proposed an adaptive fuzzy dividing frequency-control method for hybrid active power filter. In their control method, dividing frequency integral control is implemented by generalized integrator while in-time adjustment of proportional-integral coefficients is achieved by fuzzy arithmetic [8]. To implement the transform from time-domain feedback signal to frequency-involved data, wavelet theory is an attractive approach. Wavelet transform has been considered as an ideal tool for signal analysis and image processing. It has many advantages over transforms based on fourier theory, such as multiresolution in frequency domain and reducing signal correlation [9]. The fast algorithm of wavelet transform also makes it feasible in real-time control. Parvez and Gao proposed a wavelet-based multiresolution PID controller and shown its better performance than PID to provide smooth control signal, better disturbance, and noise rejection [10]. Khan and Rahman proposed a wavelet-PID controller for interior permanent-magnet motor drives and verified its effectiveness via comparison with conventional fixed-gain controllers at different dynamic operating conditions [11]. They also applied this kind of wavelet-based MRPID controller in control of benchmark thermal system and battery storage system, and got obvious effect [12,13]. Daya et. al. proposed a multiresolution controller for robust speed control of induction motor. Their controller, which is a hybrid of discrete wavelet transform (DWT) and self-tuning fuzzy logic algorithm, is validated effective and higher performance over conventional controllers [14]. Dang et al. proposed a control method based on wavelet neural network for the tracking performance of permanent magnet linear synchronous motor seriously influenced by disturbances [15]. Liu and Suh proposed an nonlinear time-frequency controller based on DWT and filtered-x LMS algorithm to minimize the vibration adaptively for AMB system [16].

In this paper, a frequency dividing control method is proposed for AMB-rotor system. The control scheme is implemented using Discrete Wavelet Transform (DWT) and PID control. First, the model of a 4-DOF AMB-rotor system is established. Then a frequency dividing controller is utilized. The controller consists of 3 main part: down sampling operation with memory to generate suitable input signal, filter banks based on Daubechies wavelet and mallat algorithm for DWT / IDWT, and a group of PID controllers for multi-frequency control. The number of frequency decomposition bands can be set flexibly and the parameters of PID controllers can be adjusted separately. Finally, the rotor dynamics are simulated in 3 different cases (basic motion, step response and circle orbit) and the vibration is analyzed to validate the control effect of the proposed method.

II. AMB-ROTOR DYNAMICS

As usual, the axial motion is not considered in radial motion study of AMB [17]. A horizontal rotor system with 2 AMBs is shown in Figure 1.

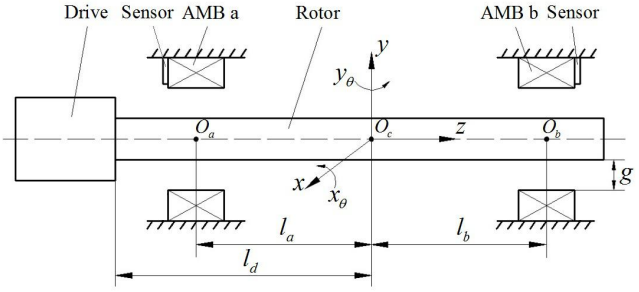

Figure 1. System with rigid rotor and AMBs

O_c is the center of rotor with the coordinates $\boldsymbol{x_c}=[x_c,x_\theta,y_c,y_\theta]^T$. Neglecting the small misalignment between actuators and sensors, $\boldsymbol{x}=[x_a,x_b,y_a,y_b]^T$ is rotor displacement at AMB position detected by sensors. The rotor is assumed to be rigid and symmetrical, so the dynamic model of this 4-DOF AMB-rotor system can be expressed as

$$\begin{aligned} \boldsymbol{M}\ddot{\boldsymbol{x}}_c + \boldsymbol{G}\dot{\boldsymbol{x}}_c &= \boldsymbol{B}\boldsymbol{F}_b + \boldsymbol{F}_r + \boldsymbol{T}_d\boldsymbol{F}_d \\ \boldsymbol{x} &= \boldsymbol{T}\cdot\boldsymbol{x}_c \end{aligned} \tag{1}$$

$$\boldsymbol{M}=\begin{bmatrix} M & 0 & 0 & 0 \\ 0 & I_x & 0 & 0 \\ 0 & 0 & M & 0 \\ 0 & 0 & 0 & I_y \end{bmatrix}, \boldsymbol{G}=\begin{bmatrix} 0 & 0 & 0 & 0 \\ 0 & 0 & 0 & I_z\omega \\ 0 & 0 & 0 & 0 \\ 0 & -I_z\omega & 0 & 0 \end{bmatrix},$$

$$\boldsymbol{B}=\begin{bmatrix} 1 & 1 & 0 & 0 \\ 0 & 0 & -l_a & l_b \\ 0 & 0 & 1 & 1 \\ l_a & -l_b & 0 & 0 \end{bmatrix}, \boldsymbol{T}=\begin{bmatrix} 1 & 0 & 0 & l_a \\ 1 & 0 & 0 & -l_b \\ 0 & -l_a & 1 & 0 \\ 0 & l_b & 1 & 0 \end{bmatrix}, \tag{2}$$

$$\boldsymbol{F}_r=[e_r m\omega^2\cos(\omega t),\quad 0,\quad e_r m\omega^2\sin(\omega t)-mg,\quad 0]^T$$

where M is the mass of rotor, I_x / I_y and I_z are rotary inertia of axis x/y and axis z respectively, ω is the angular speed of rotation around axis z, l_a / l_b is the distance between AMB a/b and rotor center, $\boldsymbol{F_b}=[F_{xa},F_{xb},F_{ya},F_{yb}]^T$ is active control force of AMBs, e_r is eccentric error of rotor, $\boldsymbol{F_d}$ is the disturbance and $\boldsymbol{T_d}$ is its transformation matrix.

The structure of AMBs is a common structure of 8 poles. The magnetic force on each pole is calculated as

$$F_m = k(\frac{i}{g})^2 \tag{3}$$

where k is the electromagnetic coefficient calculated by electromagnetic parameters, i is the pole current and g is the air gap.

The AMBs are differential driven, so the magnetic force at each direction is :

$$\begin{aligned} F_{AMB} &= k\cos\alpha[(\frac{i_0-i_c}{g_0-x})^2-(\frac{i_0+i_c}{g_0+x})^2] \\ &\approx k\cos\alpha(\frac{4i_0^2}{g_0^3}x-\frac{4i_0}{g_0^2}i_c)=k_s x-k_i i_c \end{aligned} \tag{4}$$

$$k_s = k\frac{4i_0^2}{g_0^3}\cos\alpha, k_i = k\frac{4i_0}{g_0^2}\cos\alpha \tag{5}$$

where α is the angle of pole, i_0 /i_c is the bias current / control current respectively, g_0 is the rated air gap, x is the rotor displacement at AMB position, and k_s /k_i is the displacement coefficient / the current coefficient respectively.

Power amplifier and signal feedback are simplified and considered as one-order lowpass filter respectively.

$$\dot{\boldsymbol{x}}_{pa}+\frac{1}{\tau_p}\boldsymbol{x}_{pa}=\frac{K_p}{\tau_p}\boldsymbol{x}_{out} \tag{6}$$

$$\tau_p=\frac{1}{2\pi f_p} \tag{7}$$

$$\dot{\boldsymbol{x}}_{in}+\frac{1}{\tau_f}\boldsymbol{x}_{in}=\frac{K_f}{\tau_f}\boldsymbol{x} \tag{8}$$

where $\boldsymbol{x_{pa}}$ is the output of power amplifier, $\boldsymbol{x_{out}}$ / $\boldsymbol{x_{in}}$ is the output / input of controller, τ_p is a time constant, K_p is the gain of power amplifier, f_p is the cutoff frequency of power amplifier, τ_f is a time coefficient for time delay, and K_f is the overall gain between sensor and controller.

III. FREQUENCY DIVIDING CONTROLLER

A. Process of frequency dividing

Wavelet theory is an important tool for time-frequency analysis. DWT can extract frequency components of digital signal using filters and compose the intact original signal. Mallat pyramid algorithm, which is a common framework of fast algorithm, makes DWT convenient for application. The working process of frequency dividing via DWT using Mallat pyramid algorithm is shown in Figure 2. There are 2 steps: decomposition and reconstruction (Inverse Discrete Wavelet Transform, IDWT).

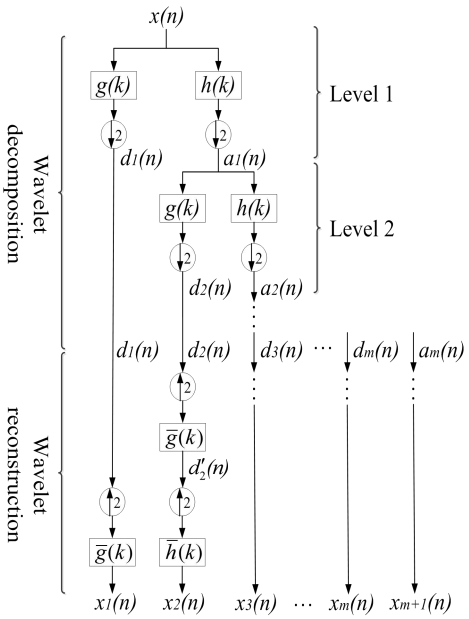

Figure 2. Working process of DWT and IDWT

The decomposition is implemented by cascaded stages of filter banks of a high-pass filter (g) and a low-pass filter (h). Down sampling operation is used to change the scale of signals. The input signal ***x(n)*** passes through the first filter bank and is decomposed to the details ***d1(n)*** by high-pass filter and the approximations ***a1(n)*** by low-pass filter, which constitutes the first level of decomposition. This operation can be mathematically expressed as

$$\begin{aligned} a_1(n) &= \sum_{k=0}^{N/2-1} h(k)x(2n-k) \\ d_1(n) &= \sum_{k=0}^{N/2-1} g(k)x(2n-k) \end{aligned} \tag{9}$$

$$\boldsymbol{x}_W(n) = \begin{bmatrix} \boldsymbol{d}_1(n) \\ \boldsymbol{a}_1(n) \end{bmatrix} = \boldsymbol{T}_w \boldsymbol{x}(n) \tag{10}$$

where *g(k)* / *h(k)* is weights of high-pass / low-pass filter determined by wavelet function, and ***Tw*** is the respective transform matrix.

Again, the approximations ***a1(n)*** is decomposed to the details ***d2(n)*** and the approximations ***a2(n)*** at the second level of decomposition. As the operation going on, the input signal is transformed to several series of wavelet coefficients representing components at different frequencies. So the input signal is divided by frequency.

$$\boldsymbol{x}_W(n) = \begin{bmatrix} \boldsymbol{d}_1(n) \\ \boldsymbol{d}_2(n) \\ \vdots \\ \boldsymbol{d}_m(n) \\ \boldsymbol{a}_m(n) \end{bmatrix} = \boldsymbol{T}_{Wm} \cdots \boldsymbol{T}_{W2} \boldsymbol{T}_{W1} \boldsymbol{x}(n) \tag{11}$$

Then in the step of reconstruction, the series of wavelet coefficients are processed respectively by the inverse operation as IDWT, and tine series representing components at different frequency ***x1(n)***,***x2(n)***,...,***xm+1(n)*** are got. Hence The input ***x(n)*** is losslessly divided:

$$\boldsymbol{x(n)} = \sum_{i=1}^{m+1} \boldsymbol{x}_i(\boldsymbol{n}) \tag{12}$$

B. Parameters selection of DWT

The choice of wavelet function from plenty of available ones doesn't have a settled solution. An object function can be set to select an optimum wavelet function [18,19]. Wavelets of the Daubechies family have been verified to be great and are widely used [20], so db4 of the Daubechies family is selected in this paper.

The number of decomposition level also influences the effect of frequency dividing. It can be set based on object function [11,19] or the target frequency bands to divide.

The length of input signal *L* should satisfy equation (13) and *L* is usually set to be a form of 2^N.

$$L \geq \frac{1}{2}[(2^m - 1)(F-1)+1] \tag{13}$$

where *m* is the number of decomposition level and *F* is the size of filter.

Enough size of signal ensures the accuracy of DWT, while lengthy data slows down the operation. So the length of input should be set appropriate for the scheme.

C. Schematic of controller

The schematic of the proposed controller and AMB-rotor system is shown in Figure 3. The target position of rotor center ***Re*** and the feedback displacement signal ***x*** detected by sensors are the inputs of controller and are used to obtain the error ***e***. Then the error ***e*** is processed by down sampling and memory to form a time series [***e***]. The operation of down sampling and the adjustment of its rate help to produce a integrated signal with suitable scale in frequency domain. Then this series is divided to several error series at different frequency via DWT and IDWT. Each errors at different frequency ***e1*** ,***e2*** , ... , ***em+1*** are processed by a P (Proportion) controller with respective gain K_{P1}, K_{P2} , ... , K_{Pm+1}. Simultaneously, the original error ***e*** is processed by a ID (Integration-Differentiation) controller. Finally, the results are added together to generate the output signal of controller ***ic***. From the control current ***ic*** via the power amplifier, the pole current ***i*** is produced and acted on AMB to generate active magnetic forces ***FAMB*** to support the rotor.

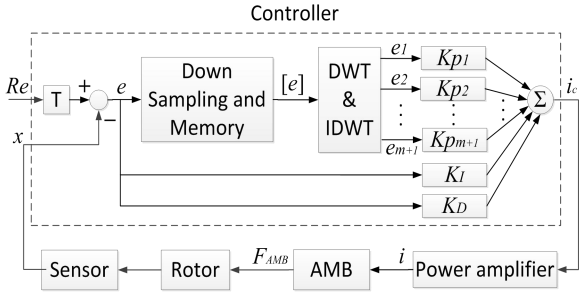

Figure 3. Block diagram of controller and system

$$\boldsymbol{e(k)} = \sum_{i=1}^{m+1} \boldsymbol{e_i(k)} \tag{14}$$

$$\boldsymbol{i_c} = \sum_{i=1}^{m+1} K_{Pi}\boldsymbol{e_i} + K_I \int_0^t \boldsymbol{e}dt + K_D d\,\frac{\boldsymbol{e}}{dt} \tag{15}$$

To the discrete signal, the output of controller is

$$\boldsymbol{i_c}(k) = \sum_{i=1}^{m+1} K_{Pi}\boldsymbol{e_i}(k) + K_I \sum_{l=0}^{k} \boldsymbol{e}(l)T_s + K_D\,\frac{\boldsymbol{e}(k)-\boldsymbol{e}(k-1)}{T_s} \tag{16}$$

where k means the present moment and T_s is the sampling period.

IV. SIMULATION RESULTS

A. Parameter Setting

The simulation is implemented in the *MATLAB-Simulink* environment with 10 kHz sample frequency. The parameters of the AMB-rotor system are given in Table 1 and the parameters of controller are given in Table 2. The disturbance forces are set as hybrid sine waves from the motor drive at half, single and double frequency of rotational speed and white noise.

Table 1. Parameters of AMB-rotor system

Name of parameter	Symbol	Value
Mass of rotor	M	2 kg
Rotational speed	n	10000 r/min
Distance between AMB a and rotor center	l_a	100 mm
Distance between AMB b and rotor center	l_b	100 mm
Distance between F_d and rotor center	l_d	150 mm
Rotary inertia of axis x/y	I_x / I_y	0.024 kg·m^2
Rotary inertia of axis z	I_z	0.001 kg·m^2
Eccentric error	e_r	5×10^{-6} m
Rated air gap	g_0	0.8 mm
Constant of magnetic force	k	3.14×10^{-6}
Angle of pole	α	π/8 rad
Bias current	i_0	2 A
Cutoff frequency of Power amplifier	f_p	1000 Hz
Time coefficient of sensor	τ_f	0.1 ms

Table 2. Parameters of controller.

Controller	Parameters
PID	K_P=1.5×10^4, K_I=1×10^5, K_D=25
Proposed	L=128, m=3, Down sampling rate: 10, Wavelet: db4, K_{P1}=1.6×10^4, K_{P1}=1.4×10^4, K_{P1}=1×10^4, K_{P4}=0.5×10^4, K_I=1×10^5, K_D=25

B. Results Analysis

The proposed controller is compared with a common PID controller. The motion orbit of rotor center using different controllers is shown in Figure 4. It can be seen that the motion is not in a tidy circular orbit because of the disturbance forces and the proposed controller performs better with smaller radial displacement.

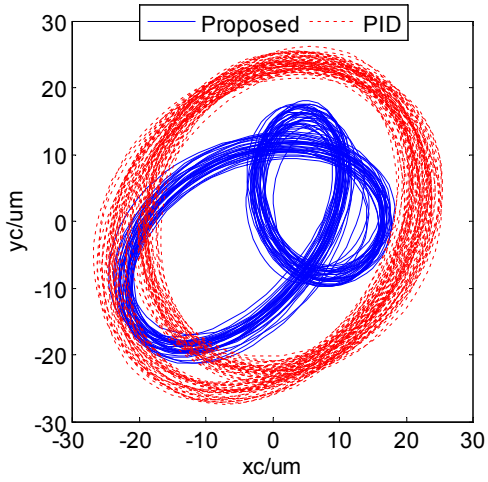

Figure 4. Motion orbit of rotor center

The result of real time decomposition of error via wavelet is shown in Figure 5. *e1* to *e3* is the details from the respective level and *e4* is the approximations. It is clear that the high frequency component is divided in succession and the original signal is finally decomposed to 4 components in different frequency band.

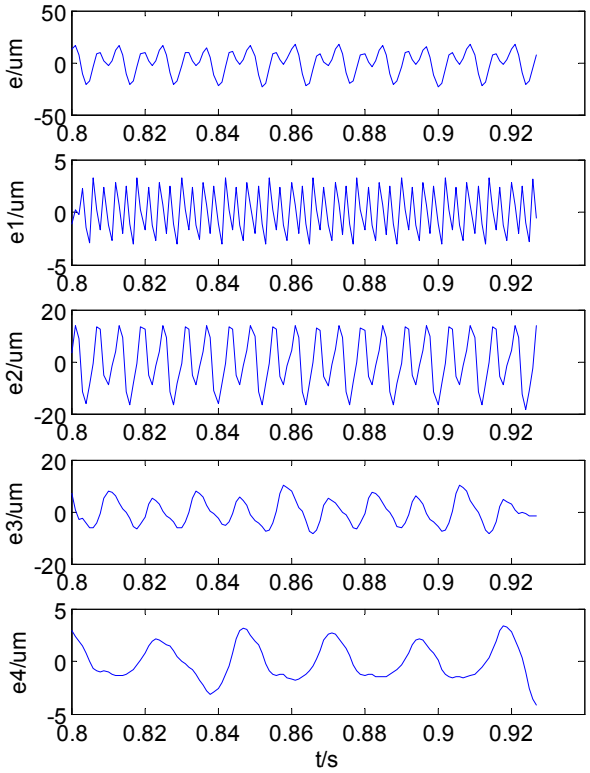

Figure 5. Error decomposition of x_a

The steady error comparison is shown in Figure 6 and Table 3. We can see an obvious improvement by the proposed controller in both maximum error and RMSE (Root-Mean-Square Error).

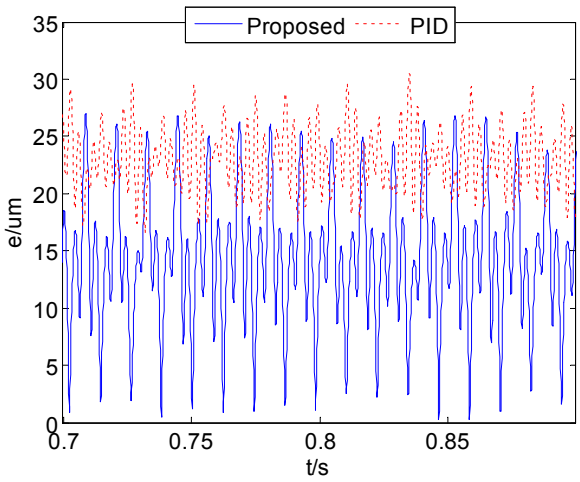

Figure 6. Steady error of rotor center

Table 3. Steady error Analysis

Error	Proposed	PID
Max/μm	26.8	30.5
RMSE/μm	15.6	23.1

In the second case, the rotor is set to implement a step response. A displacement of 0.1 mm at 0.2 s is set at y direction. The response of rotor motion at y direction is shown in Figure7. The transient response time by the proposed controller is less than 0.2 s, much quicker than the response by PID controller. Same with previous case, the precision of the proposed controller is better with smaller steady error.

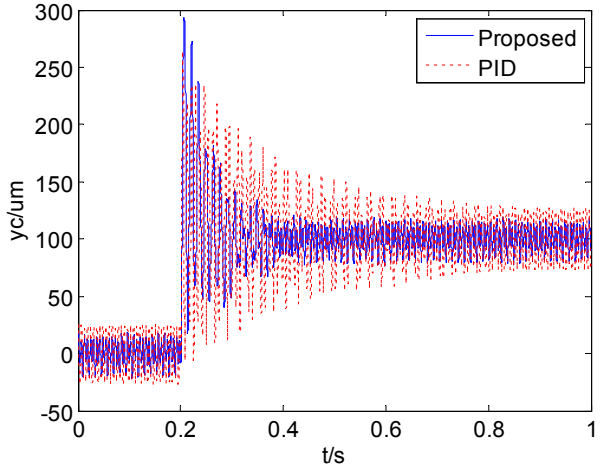

Figure 7. Step response at y direction

In the third case, the rotor is expected to run a circle orbit with radius of 0.1 mm. So the displacement of rotor at x /y direction is controlled to track a sine curve. The motion of rotor at x direction is shown in Figure 8. It can be seen that in tracking response, the proposed controller performs slightly better than PID controller with less phase lag. While in precision, the proposed controller has a significant advantage, which can also be indicated in Figure 9. Figure 9 shows the position error comparison of the circle orbit. The maximum position error and the average position error by the proposed controller is nearly half the error by PID controller.

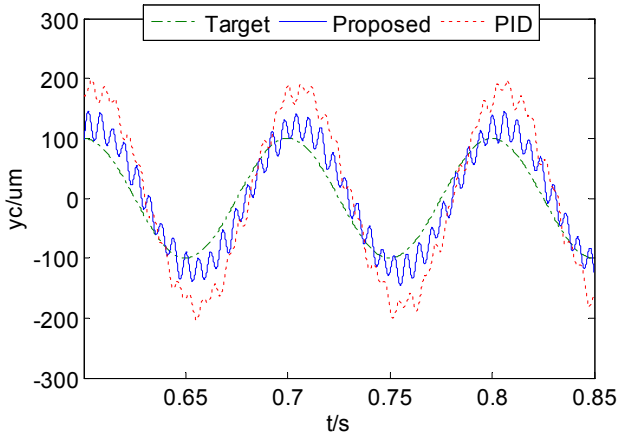

Figure 8. Sine tracking at x direction

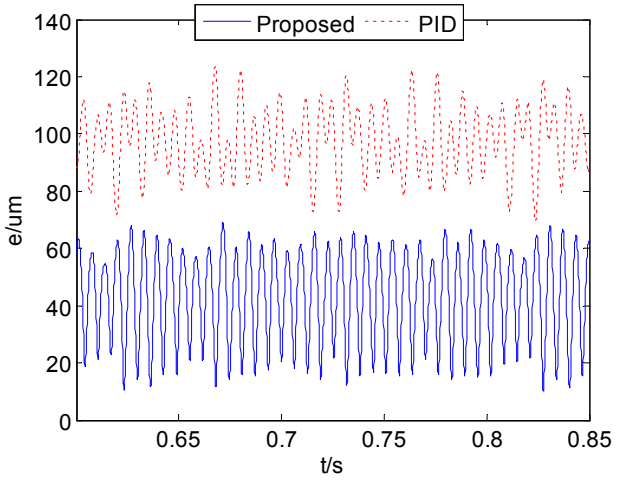

Figure 9. Steady error of circle orbit

In the above 3 cases, the proposed controller shows its effect in both control precision and response. The parameters of the proposed controller are set similar to contrastive PID controller to maintain congruent mechanical properties like equivalent stiffness and equivalent damping. While the decline of proportion gain for high frequency component reduces the over response of high-frequency component and reduces damage from disturbance and noise, to complete a better control performance..

V. CONCLUSIONS

In this paper, a wavelet-based frequency dividing control method is proposed and designed for active magnetic bearing system. Frequency dividing control is implemented by wavelet transform (DWT and IDWT) and each decomposed signal of the error at different scales is processed by an independent Proportion controller. The scale of frequency dividing is designed by down sampling operation and choice of

decomposition level. The proposed controller is validated by simulation in different cases. It is found to have a better control performance than conventional PID controller with better precision and quicker response while maintain congruent mechanical properties.

VI. ACKNOWLEDGMENTS

This work is supported by the National Natural Science Foundation of China (Grant No. 11772103 and Grant No. 61304037).

REFERENCES

[1] G. Schweitzer, and E. H. Maslen, *Magnetic bearings: theory, design, and application to rotating machinery*, Springer, Verlag Berlin Heidelberg, pp.15-23, 2009.

[2] Y. Okada, and K. Nonami, "Research trends on magnetic bearings : overview of the 8th International Symposium on Magnetic Bearings (ISMB-8) (Magnetic Bearing)," *Jsme International Journal*, vol. 46, no. 2, pp. 341-342, 2004.

[3] SL. Lei, and A. Palazzolo, "Control of flexible rotor systems with active magnetic bearings," *Journal of Sound & Vibration*, vol. 314, no. 1, pp. 19-38, 2008.

[4] CC. Wei, Y. Wang, SQ. Chen, and Q. Liang, "Control of an electromagnetic suspension vibration isolator based on block normalized LMS algorithm," *Journal of Vibration & Shock*, vol. 31, no. 18, pp. 100-103, 2012.

[5] K. Plaza, and M. Pawelczyk, "Active vibration damping in a magnetic levitation system using LMS algorithm," *International Congress on Sound and Vibration 2009*, vol. 8, pp. 4834-4841, 2009,.

[6] MS. Kang, and WH. Yoon, "Acceleration feedforward control in active magnetic bearing system subject to base motion by filtered-X LMS algorithm," *IEEE Transactions on Control Systems Technology*, vol. 14, no. 1, pp. 134-140, 2005.

[7] A. Tzes, and K. Kyriakides, "A hybrid frequency-time domain adaptive fuzzy control scheme for flexible link manipulators," *Journal of Intelligent & Robotic Systems*, vol. 10, no. 3, pp. 283-300, 1994.

[8] A. Luo, ZK. Shuai, WJ. Zhu, RX. Fan, and CM. Tu, "Development of hybrid active power filter based on the adaptive fuzzy dividing frequency-control method," *IEEE Transactions on Power Delivery*, vol. 24, no. 1, pp. 424-432, 2009.

[9] RQ. Yan, RX. Gao, and X. Chen, "Wavelets for fault diagnosis of rotary machines: A review with applications," *Signal Processing*, vol. 96, no. 5, pp. 1-15, 2014.

[10] S. Parvez, and Z. Gao, "A wavelet-based multiresolution PID controller," *IEEE Transactions on Industry Applications*, vol. 41, no. 2, pp. 537-543, 2005.

[11] M. A. S. K. Khan, and M. A. Rahman, "Implementation of a new wavelet controller for interior permanent-magnet motor drives," *IEEE Transactions on Industry Applications*, vol. 44, no. 6, pp. 1957-1965, 2008.

[12] M. A. S. K. Khan, and M. A. Rahman, "Implementation of a wavelet-based MRPID controller for benchmark thermal system," *IEEE Transactions on Industrial Electronics*, vol. 57, no. 12, pp. 4160-4169, 2010.

[13] M. A. S. K. Khan, and M. A. Rahman, "Implementation of wavelet-based controller for battery storage system of hybrid electric vehicles," *IEEE Transactions on Industry Applications*, vol. 47, no. 5, pp. 2241-2249, 2011.

[14] J. L. F. Daya, V. Subbiah, and P. Sanjeevikumar, "Robust speed control of an induction motor drive using wavelet-fuzzy based self-tuning multiresolution controller," *International Journal of Computational Intelligence Systems*, vol. 6, no. 4, pp. 724-738, 2013.

[15] XJ, Dang, XP. Xu, XM. Yu, and H. Jiang, "Control for PMLSM based on wavelet neural network," *Electric Machines & Control*, vol. 17, no. 1, pp. 43-50, 2013.

[16] MK. Liu, and C.S. Suh, "Active magnetic bearings for high speed spindle design with nonlinear time-frequency control," *ASME 2015 International Mechanical Engineering Congress and Exposition 2015*, pp. V04BT04A023, 2015.

[17] G. Schweitzer, and E. H. Maslen, *Magnetic bearings: theory, design, and application to rotating machinery*, Springer, Verlag Berlin Heidelberg, pp.188-190, 2009.

[18] E. Y. Hamid, and Z. I. Kawasaki,"Wavelet-based data compression of power system disturbances using the minimum description length criterion," *IEEE Transactions on Power Delivery*, vol. 17, no. 2, pp. 460-466, 2001.

[19] C.S. Suh, and M. K. Liu.,*Control of Cutting Vibration and Machining Instability*, John Wiley & Sons Ltd, Chichester,United Kingdom, pp. 153-154, 2013.

[20] S. Mallat, *A Wavelet Tour of Signal Processing: The Sparse Way*, Academic press, Burlington, MA, pp. 212-222, 2008.